Thermosensitive Hydrogels of BAB Triblock Copolymers Exhibiting Gradually Slower Exchange Dynamics and an Unexpected Critical Reorganization Temperature Upon Heating

Noémie Coudert, Clément Debrie, Jutta Rieger, Taco Nicolai, Olivier Colombani

Thermo-sensitive hydrogels of BAB triblock copolymers exhibiting gradually slower exchange dynamics and an unexpected critical reorganization temperature upon heating.

Noémie Coudert,[a] *Clément Debrie,*[b] *Jutta Rieger,*[b] *Taco Nicolai,*[a] *Olivier Colombani*,*[a]

[a] Institut des Molécules et Matériaux du Mans (IMMM), UMR 6283 CNRS Le Mans Université, Avenue Olivier Messiaen, 72085 Le Mans Cedex 9, France

[b] Institut Parisien de Chimie Moléculaire (IPCM), Sorbonne Université, CNRS, UMR 8232, Polymer Chemistry Team, 4 Place Jussieu, 75252 Paris Cedex 05, France.

KEYWORDS amphiphilic block copolymer; exchange dynamics; hydration; light scattering; poly(dimethylacrylamide); RAFT; rheology; poly(methoxyethyl acrylate); thermo-responsive hydrogel; triblock.

ABSTRACT

BAB amphiphilic triblock copolymers comprising poly(methoxyethyl acrylate) (PMEA) B-blocks of variable degrees of polymerization (x = 50, 100 or 200) and a central poly(dimethyl acrylamide) (PDMAc) hydrophilic A-block with a degree of polymerization y = 400 were synthesized by RAFT polymerization and their self-assembly in water was studied by light scattering and rheology. The BAB triblocks form a transient network in aqueous solution consisting of hydrophobic B cores bridged by hydrophilic A blocks. The exchange of B blocks is fast at low temperature (10°C) and/or low x values because PMEA is not too hydrophobic. However, the PMEA blocks become more hydrophobic with increasing temperature, leading to a decrease of the exchange rate of the B blocks and to tunable thermo-thickening properties, opposite to a classical Arrhenius behavior. In contrast to many thermo-sensitive BAB triblocks that undergo an abrupt sol-gel transition above the critical solubility temperature of the B blocks, the hydrophobicity of PMEA gradually increases with T, leading to a progressive increase of the viscosity of the polymer dispersion. In addition, an unprecedented reorganization of the network was observed by rheology at a critical temperature leading to a further decrease of the exchange rate of the B blocks that is not fully reversible. These features were attributed to the progressive variation of the hydrophobic character and hydration of PMEA with temperature.

Introduction

Gels are solid-like materials consisting of two or more components[1], the main constituent being a liquid which can be water (hydrogels), an organic solvent (organogels[2-6]), an ionic liquid (ionogels[7-9]) or in some cases both water and an organic solvent (organohydrogels[10]). They can find applications in various fields including the food industry[11-13], the health sector[14-24], coatings

and sealants[23], energy[25-26] storage, enhanced oil recovery[27], organic electronics[28] or catalysis and sustainable chemistry[7] for example. Many strategies[5,12,23,29-39] exist to form gels, but a very attractive one relies on the solution self-assembly of linear BAB triblock copolymers consisting of solvophobic lateral B blocks connected to a central solvophilic A block[3,40,41]. Solvophobic cores containing several B blocks serve as physical cross-links bridged by the A blocks, resulting in a 3D-spanning network preventing or slowing down flow. One key advantage of this strategy is that tuning the solubility of the B blocks with an external stimulus affects the strength of the self-assembly between the B blocks, leading to stimuli-responsive materials. In this context, temperature-responsive hydrogels[18-22,42,] and ionogels[8] have been widely studied because the former class allows injectability[20] or controlled release of drugs[14] for biomedical applications, while the latter allows processability for applications in separation membranes, energy storage or electronics for example.

For ionogels, specific polymer-ion and cation-anion interactions allow tuning the solubility of the B blocks[9,43], leading either to B blocks exhibiting an Upper Critical Solubility Temperature (UCST) or a Lower Critical Solubility Temperature (LCST), resulting respectively in gel-sol or sol-gel transitions upon temperature increase. For hydrogels[14,18,19,22,44], hydrogen bonding of the B blocks with water is mainly responsible for the existence of UCST-type or LCST-type transitions. However, in most studies on gels formed by the self-assembly of BAB triblock copolymers in solution, B-blocks exhibiting abrupt temperature-transition behaviors have been used, resulting in an on-off reversible transition from a low viscosity liquid to a non-flowing gel[8,18-20]. This abrupt transition can be explained by the fact that the rheological properties of the physically cross-linked networks are controlled by the exchange time of the B blocks, the latter depending primarily on

their solvophobic character[40,45-48]. Hence, highly solvophobic B blocks lead to non-flowing gels because their exchange time is long compared to the experimental time window.

Rarely, hydrogels have been obtained with moderately hydrophobic and thermo-responsive B blocks which become gradually more hydrophobic with increasing temperature[49-51]. This does not result in an abrupt temperature-induced transition from a low viscosity aqueous solution to a non-flowing gel, but causes a gradual increase of the viscosity of the solution with increasing temperature. This behavior is opposite to the classical Arrhenius behavior causing a decrease of viscosity with increasing temperature [40,47,48,52]. Hietala et al. [53] prepared BAB triblock copolymers with a central atactic poly(*N*-isopropyl acrylamide) (PNIPAM) block, which remained hydrophilic below its LCST = 32°C, and lateral isotactic PNIPAM blocks, which did not exhibit any distinct LCST, but were partly hydrated at 5°C and dehydrated with increasing temperature. As a result, hydrogels exhibiting a thermo-thickening behavior were observed below 32°C: the viscosity of the solutions increased with increasing temperature, suggesting an increase of the exchange time of the B blocks with increasing temperature. Mistry et al.[49] studied BAB triblock copolymers with short poly(butylene oxide) (PBO) lateral B blocks (DP_n = 10) and a long central poly(ethylene oxide) block. An increase of the rheological relaxation time with temperature was observed. The authors attributed the phenomenon to the dispersity of the PBO blocks. It seems however more reasonable to explain these results by an increase of the hydrophobic character of the PBO blocks with temperature as reported by Castelletto et al.[54]. More recently, Tsitsilianis et al.[50] and Lauber et al.[51] studied BAB triblock copolymers with a central hydrophilic poly(dimethyl aminoethyl methacrylate) (PDMAEMA) block and lateral B blocks consisting of random copolymers of very hydrophobic *n*-butyl methacrylate and a rather hydrophilic and thermosensitive comonomer (respectively triethylene glycol methacrylate or DMAEMA). In both cases, the presence of the

thermo-sensitive comonomer imparted temperature responsiveness to the triblocks, resulting in an increase of the exchange time of the B blocks with increasing temperature. The former was studied in view of preparing injectable hydrogels exhibiting sufficiently low viscosity at 5°C for injection, but becoming gels at body temperature. Another polymer architecture has been described by Podhajecka et al.[55] who studied poly(sodium acrylate)s grafted with moderately hydrophobic poly(*tert*-butyl acrylamide). These graft copolymers formed transient networks also exhibiting an increase in viscosity with increasing temperature. The small number of systems leading to gradual increase of the viscosity with T is probably due to the rarity of intrinsically moderately hydrophobic homopolymers that are able to dehydrate progressively with increasing temperature. In these earlier studies, the effect of the length of the B blocks on the variation of the exchange time had not been investigated yet on such systems.

In this context, poly(methoxyethyl acrylate) (PMEA) is of interest. PMEA belongs to the poly(oligoethylene glycol (meth)acrylate) series[56-59], but contrary to other polymers of this series, PMEA is already hydrophobic at room temperature, because its LCST is close to 5°C.[60] Still, PMEA is significantly hydrated (~ 10 wt%) at room temperature[61,62]. Contrary to the better known PNIPAM, which dehydrates abruptly at its LCST, PMEA dehydrates progressively with increasing temperature, making it potentially suitable to design thermo-responsive hydrogels exhibiting gradual increase of their exchange time with T. Chemical gels, homopolymers or block copolymers containing PMEA[63,64] have been widely studied especially in view of the strong blood compatibility[61,62,64-69] of this polymer, which is attributed to its strong interaction with water[61,62,64-75], or for the design of self-assembled particles by Polymerization-Induced Self-assembly[76,77]. However, to the best of our knowledge, PMEA has so far not been used as B block in view of preparing transient networks exhibiting thermo-thickening properties.

In this study, we investigated the exchange dynamics of BAB triblock copolymers consisting of PMEA B-blocks of varying degrees of polymerization (x = 50, 100 or 200) and a central poly(dimethyl acrylamide) (PDMAc) hydrophilic A-block with y = 400. The polymers were prepared by Reversible Addition Fragmentation chain-Transfer (RAFT) radical polymerization and their self-assembly in aqueous solution was studied by light scattering and linear rheology. We observed that the triblock copolymers not only exhibit the targeted progressive thermo-sensitivity leading to thermo-thickening hydrogels with gradually slower exchange dynamics, but that they also show an unprecedented transient network reorganization at a critical temperature that depends on the DP_n of the B blocks.

Material and methods

1. Synthesis of the $PMEA_x$-*b*-$PDMAc_{400}$-*b*-$PMEA_x$ *triblock copolymers*

The three $PMEA_x$-*b*-$PDMAc_{400}$-*b*-$PMEA_x$ with x = 50, 100 or 200 were prepared by RAFT polymerization as described in section 1 of the Supporting Information.

2. Preparation of aqueous polymer dispersions for light scattering and rheology

Aqueous polymer samples were prepared by directly dispersing the polymer powder in deionized water (Millipore, 18 MΩ.cm) at room temperature. For samples at low polymer concentration (<10 g/L) macroscopic dissolution was achieved under stirring at room temperature overnight. The samples were then stored at least 24h in the fridge (~ 5°C) to make sure that equilibrium was reached. For higher polymer concentrations leading to highly viscous solutions or hydrogels, the samples were placed in an iced bath (~ 0°C) or in a fridge (~ 5°C) and regularly homogenized by manual shaking to speed up the dissolution process. Homogeneous samples were obtained after one to three days depending on the polymer concentration and x. They were stored in the fridge until use.

3. Static and Dynamic Light Scattering (SLS and DLS)

Light scattering measurements were done using ALV-CGS3 and ALV-CGS8 systems operating with vertically polarized He-Ne laser with a wavelength λ=633nm (ALV-GmbH, Germany) coupled with an ALV-5004 and ALV-5003 multi tau correlator system (ALV-GmbH, Germany) respectively. Samples were placed in a thermostated decalin bath that is quasi isorefractive of glass in order to lower reflections of light at the surface of the light scattering cells.

The measurements were done over a wide range of scattering wave vectors q = $6.8.10^4$ – $2.5.10^5$ cm^{-1} defined as $q = \frac{4\pi n}{\lambda} \, sin\left(\frac{\theta}{2}\right)$ (with n = 1.33 the refractive index of the solvent that is water in

the present investigation, and θ = 30-150° the angle of observation). Polymer solutions were studied by light scattering in a concentration range C = 0.1 to 3 g/L. The temperature was controlled between 10 and 50°C by a thermostatic bath to within ±0.2 °C. All solutions were filtered through Acrodisc GHP 0.45 µm pore size filters before measurement.

Dynamic Light Scattering (DLS). The Siegert equation $g_2(t) = 1 + \beta g_1^2(t)$, where β is the spatial coherence factor, was used to determine the electric field autocorrelation function, $g_1(t)$, from the measured normalized autocorrelation function of the scattered light intensity, $g_2(t)$. The relaxation time (τ) distributions, A(τ), were extracted from $g_1(t)$ using the REPES[78,79] routine (equation 1).

$$g_1(t) = \int A(\tau) \exp\left(-\frac{t}{\tau}\right) d\tau \qquad \text{equation (1)}$$

In the concentration range investigated, a single relaxation mode was observed. The cooperative diffusion coefficient, D, was determined from the average relaxation rate : $D = \frac{\langle \tau^{-1} \rangle}{q^2}$ and is linked to the z-average hydrodynamic radius R_h of the solute using the Stokes-Einstein equation (equation 2).

$$R_h = \frac{kT}{6\pi\eta D} \qquad \text{equation (2)}$$

With k = 1.38×10^{-23}J/K Boltzmann's constant, η the solvent (water) viscosity which depends on temperature, T.

Static Light Scattering (SLS). The Rayleigh ratio, R_θ, was calculated according to equation 3.

$$R_\theta = \frac{I_{solution}(\theta) - I_{solvent}(\theta)}{I_{toluene}(\theta)} \left(\frac{n_{solvent}}{n_{toluene}}\right)^2 R_{toluene} \qquad \text{equation (3)}$$

where $I_{solution}$, $I_{solvent}$ and $I_{toluene}$ are the average intensities scattered respectively by the solution, the solvent, and the reference (toluene). The Rayleigh ratio of the reference is $R_{toluene}$ = 1.35 x 10^{-}

^{5} cm^{-1}, and the refractive indexes of the reference and the solvent (water) are respectively $n_{toluene}$ = 1.496 and $n_{solvent}$ = 1.333.

The apparent molar mass (M_{app}) of the solute at concentration C was calculated from the Rayleigh ratio of the solution according to equation 4.

$$R_\theta = KCM_{app}S(q) \qquad \text{equation (4)}$$

where S(q) is the structure factor and K a constant defined in equation 5.

$$K = \frac{4\pi^2 n_{solvent}^2}{\lambda^4 N_A}\left(\frac{\partial n}{\partial c}\right)^2 \qquad \text{equation (5)}$$

where $\partial n/\partial c$ is the specific refractive index increment of the solute and N_A is Avogadro's number. A refractive index increment $\partial n/\partial c$ = 0.15 mL/g was measured with a differential refractometer (Oprilab rEX – Wyatt Technology Corporation) at λ = 633 nm for one of the triblock copolymers with solutions at a concentration between 1 and 5 g/L.

In dilute solutions (C = 0.1-3 g/L), one single population of scatterers was observed by DLS for all x and T investigated (see data for x = 100 within the T-range of investigation Figure S4 SI). M_{app} exhibited no significant angular dependency, implying that S(q) ~ 1 and that the radius of gyration R_g of the scatterers was too small to be determined accurately (R_g < 20 nm). Moreover, M_{app} (resp. R_{app}) did not vary with C in this concentration range implying that it represented the true weight average molecular weight of the scatterers, M_w, (resp. true hydrodynamic radius, R_h) with an uncertainty of about 10%.

The aggregation number, N_{agg}, corresponding to the number of B blocks within the self-assembled structures, was determined as $N_{agg} = \frac{2.M_w}{M_{w,triblock}}$ taking into account that each triblock copolymer possesses two B blocks.

4. Rheology

Rheological measurements were carried out using a DHR3 rheometer equipped with cone –plate geometries (angle = 1°, 2°; diameter = 20, 40 mm truncation = 28, 59 µm); chosen depending on the sample viscosity. Temperature was controlled by a Peltier system.

Samples were loaded onto the rheometer at 10 or 20°C and homogenized by shearing (3 rad/s). Silicon oil was used to cover the free sample surface in order to avoid water evaporation during the measurements. Oscillatory frequency-sweeps shear measurements were done in the linear response domain between 0.01-10 Hz at temperatures ranging from 5 to 60°C. The evolution of the system after a change of temperature was determined by measuring the elastic modulus G' (Pa) and loss modulus G'' (Pa) as a function of time after increasing as fast as possible the temperature from 10°C to the target temperature. It took about one minute to reach the target temperature (the required time is indicated in the figures' caption). Viscosities were determined by oscillatory shear or shear flow measurements.

The elastic modulus, G_e was taken as the value of G' at f = 100.f_r (f_r = cross-over frequency where G' = G'') where most bridging chains could not relax. The formation of master curves by frequency-temperature superposition enabled us to obtain values of G_e when they could not be determined directly within the measured frequency range. G_e was compared to G_{e_ideal} which corresponds to the elastic modulus of an ideal network where all BAB chains are elastically active (equation 6).

$$G_{e\_ideal} = \nu_{ideal}.k.T = \frac{C.N_A}{M_n}.k.T \qquad \text{(equation 6)}$$

with ν_{ideal} the total number concentration of $PMEA_x$-*b*-$PDMAc_{400}$-*b*-$PMEA_x$ chains, N_A the Avogadro's number, C the polymer concentration in g/L and M_n the number average molecular weight of the polymer.

Results and discussion

1. Synthesis of the PMEA$_x$-*b*-PDMAc$_{400}$-*b*-PMEA$_x$ triblock copolymers.

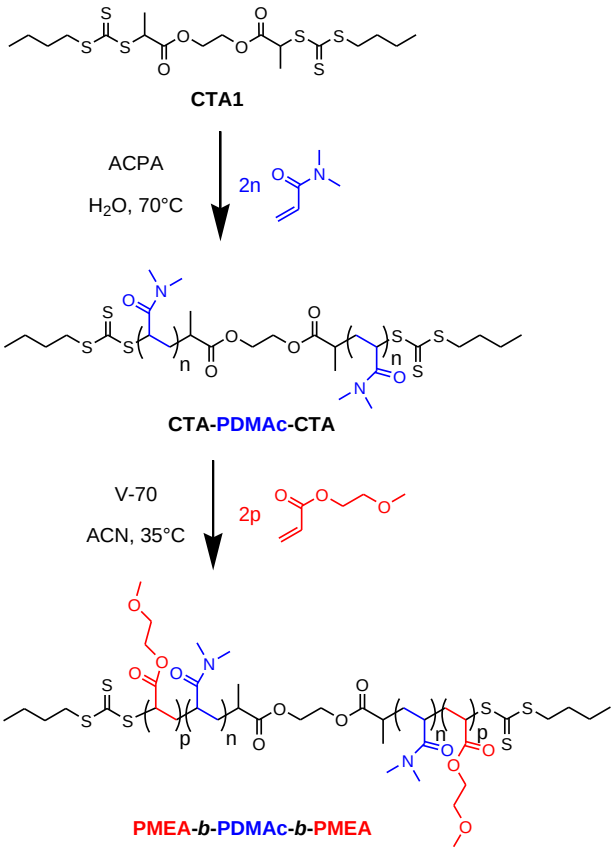

Scheme 1**.** Synthesis route for the PMEA$_x$-*b*-PDMAc$_{400}$-*b*-PMEA$_x$ triblock copolymers obtained by the extension of the bifunctional CTA-PDMAc$_{400}$-CTA macroCTA in solution.

Three PMEA$_x$-*b*-PDMAc$_{400}$-*b*-PMEA$_x$ triblock copolymers exhibiting a degree of polymerization x = 50, 100 or 200 for the PMEA block and 400 for the PDMAc block were prepared by RAFT polymerization in solution according to Scheme 1, see details in section 1 of the Supporting Information. Briefly, a bifunctional trithiocarbonate (CTA1) was used to control the polymerization of DMAc with a molar ratio $[DMAc]_0/[CTA1]_0/[ACPA]_0$ ~ 441/1/0.10 (see Table S1). The polymerization of DMAc was started in bulk at 60°C for 20 min to ensure the

solubility of CTA1. Then, water was added and the polymerization was allowed to proceed at 70°C until 90% monomer conversion to reach the targeted degree of polymerization of the central PDMAc block. After purification by dialysis against water and freeze-drying, the bifunctional CTA-PDMAc$_{400}$-CTA macroCTA was used to control the polymerization of MEA in ACN solution at 35°C. The [MEA]$_0$/[macroCTA]$_0$ ratio was adapted to reach the desired x value at around 30% conversion, where the reaction was stopped. Well-defined triblock copolymers PMEA$_x$-*b*-PDMAc$_{400}$-*b*-PMEA$_x$ with the expected degrees of polymerization of the blocks and a rather low dispersity ($Đ$ ~ 1.1-1.2) were eventually obtained (see details in section 1 of the Supporting Information and Table S2).

2. Characterization of the self-assembly in aqueous medium

2.1. Self-assembly at the nanometric scale.

For x = 50, 100 and 200, the triblock copolymers dissolved rapidly in water at 10°C. A fourth triblock copolymer with x = 300 (data not shown) was also synthesized, but it did not fully dissolve even after a prolonged period of time and was not further investigated. The self-assembly in water of the other PMEA$_x$-*b*-PDMAc$_{400}$-*b*-PMEA$_x$ triblock copolymers with x = 50, 100, 200 was investigated at low concentrations (0.1-3 g/L, where interactions can be neglected) as a function of T and x by static (SLS) and dynamic (DLS) light scattering.

Figures 1a) and b) present the evolution of the aggregation number N_{agg} (extracted from M_w, see experimental section, SI section 2 and Figure S5) and R_h of the self-assemblies formed by the BAB triblock copolymers as a function of T for x = 50, 100 and 200. The dimensions of the particles were compatible with those of small spherical micelles. At a given temperature < 30°C, the extent of aggregation varied in the order x = 200 > x = 100 > x = 50 (see Figure 1b and in SI Figure S6), which is compatible with an increased hydrophobic character with longer B blocks. For x = 100

and 200, N_{agg} and R_h do not significantly vary with T between 10°C and 50°C. On the contrary, for x = 50, N_{agg} is close to 2 (corresponding to one unimer) at 10°C, but the polymer chains progressively associate (N_{agg} increases with T), especially between 10 and 20°C until it reaches an N_{agg} close to that of x = 100 above 20°C.

a)

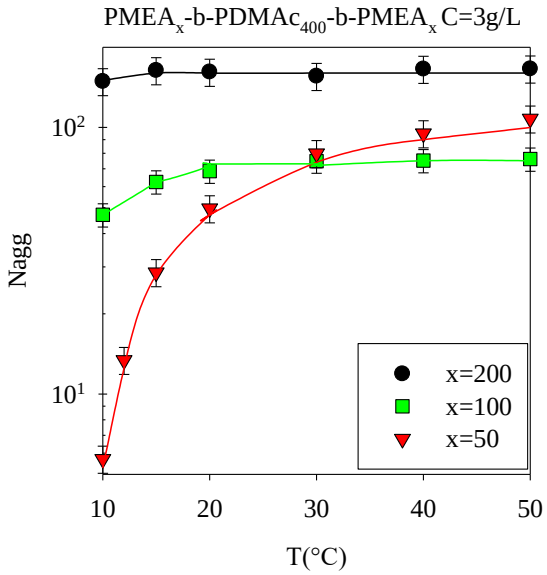

b)

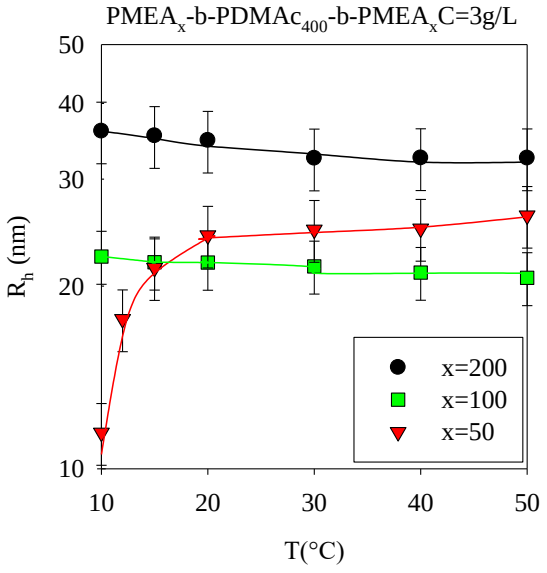

Figure 1. Evolution of a) N_{agg}, b) R_h (nm) at different temperatures (°C) for the three triblock copolymers. Lines are guides to the eyes.

2.2. Transient networks with T and x-dependent exchange dynamics

The self-assembly of $PMEA_x$-*b*-$PDMAc_{400}$-*b*-$PMEA_x$ triblock copolymers (with x = 50, 100 and 200) was further characterized by rheology at higher concentrations (C = 5-100 g/L), where transient networks eventually formed. Temperature sweeps revealed that the networks underwent a peculiar reorganization phenomenon above a critical transition temperature, T_c. This phenomenon affects the behavior of the networks and is discussed in detail in section 2.3. In the present section, the rheological properties of the networks are only presented below T_c. Note that T_c varies with x (T_c ~ 55°C, 35°C and 13°C respectively for x = 50, 100 and 200), explaining why the temperature-range presented here differs depending on x.

Formation of a transient network. The evolution of the viscosity of aqueous dispersions of the polymers as a function of concentration was first investigated for the three different x values and for different temperatures (see Figure S7). Figure 2a shows a representative example corresponding to x = 100 and T = 20°C. At low polymer concentration (C < 20 g/L), the viscosity is close to that of pure water, but above about 30 g/L it increases exponentially with increasing concentration. This behavior is characteristic of the formation of a 3D-spanning network of bridging micelles[40,45,80], which occurs above the percolation concentration (C_p, where C_p ~30g/L for x=100 and T=20°C). The viscosity remains measurable at 20°C even at the highest concentrations investigated, suggesting that the B blocks are always able to exchange within a reasonable time-scale, allowing the transient (= dynamic) network to reorganize and the system to flow.

a)

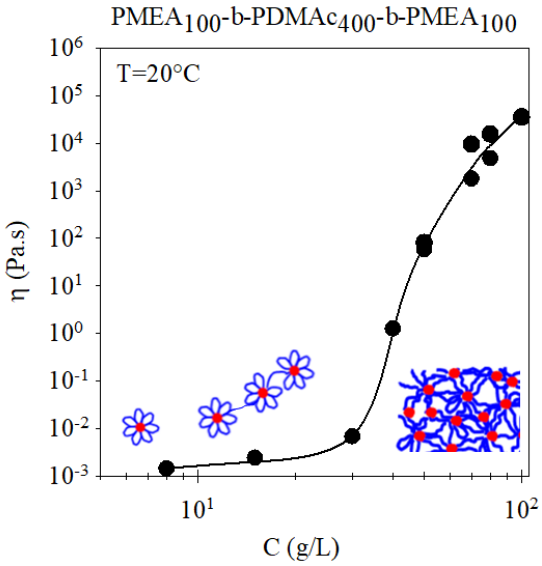
PMEA100-b-PDMAc400-b-PMEA100
T=20°C
η (Pa.s)
C (g/L)

b)

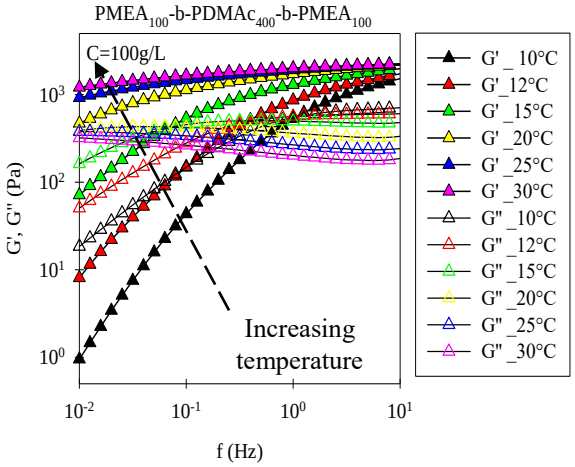
PMEA100-b-PDMAc400-b-PMEA100
C=100g/L
Increasing temperature
G', G'' (Pa)
f (Hz)
G' _10°C
G'_12°C
G' _15°C
G' _20°C
G' _25°C
G' _30°C
G'' _10°C
G'' _12°C
G'' _15°C
G'' _20°C
G'' _25°C
G'' _30°C

c)

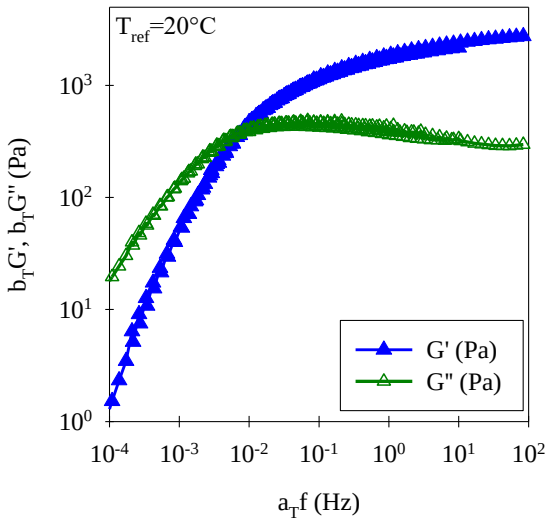

Figure 2. $PMEA_{100}$-*b*-$PDMAc_{400}$-*b*-$PMEA_{100}$. a) newtonian viscosity (Pa.s) as function of C (g/L) at 20°C. The inserted drawings represent the expected behavior at the nanometric scale: individual flower-like micelles with a red hydrophobic core consisting of PMEA blocks and blue hydrophilic "petals" of PDMAc at low concentrations; bridged micelles at moderate concentrations; and a 3D-spanning network at $C > C_p$; b) Frequency dependencies of the storage G' (Pa) and loss G''(Pa) moduli at different temperatures (°C) and c) corresponding temperature-master curves at T_{ref} = 20°C. a_T and b_T represent, respectively, the horizontal and vertical shift factors. Lines are guides to the eye.

Dynamic rheological measurements were conducted above C_p (determination of C_p as function of x and T is presented below, see Figure 4. C_p is never higher than 30 g/L) to probe quantitatively the exchange rate of the B blocks between hydrophobic cores. Figure 2b represents the evolution of the elastic (G') and loss (G") moduli as a function of frequency at different temperatures for x = 100 and at C = 100 g/L, i.e. well above C_p. The data at different T could be

superimposed to form a master curve using horizontal and vertical shift factors, see Figure 2c. The cross-over frequency (f_r) between a liquid (G' < G") and a solid (G' > G") behavior was used to define the characteristic relaxation time of the network $\tau_r = \frac{1}{2\pi f_r}$. The relaxation is caused by exchange of the B blocks among different hydrophobic cores[40,45,46]. The relaxation of the transient network is characterized by a distribution of relaxation times as was already observed for other BAB triblock copolymers and can be explained by the dispersity in length of the B blocks[40,80-82]. For x = 50, 100 and 200, the same qualitative behavior was observed for all $T < T_c$ and $C > C_p$ investigated, allowing the construction of a single master curve (see Figure S8 SI) and implying that a transient network was formed with a similar relaxation mechanism independent of x and T.

Dependence of the percolation concentration on T and x. According to the theory of rubber elasticity[83], the elastic modulus at the rubbery plateau (G_e, determined as described in the experimental part) is proportional to the number of elastically active chains in the network that is the number of BAB chains forming a bridge between two micellar cores connected to the network (equation 7).

$$G_e = \nu.k.T \qquad \text{(equation 7)}$$

with G_e in Pa, ν the number concentration of elastically active chains (number of molecules.m^{-3}), k Boltzmann's constant (m^2.kg.s^{-2}.K^{-1}) and T the absolute temperature (K).

a)

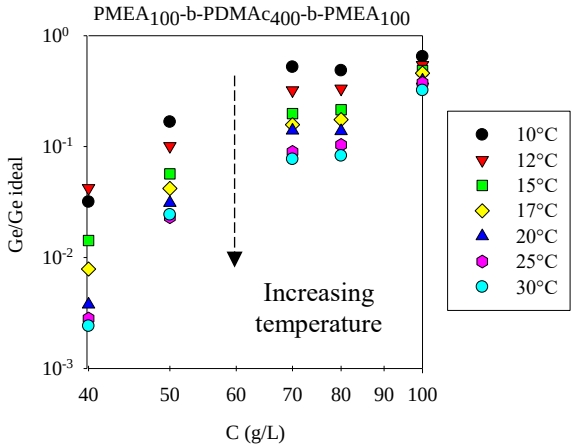

b)

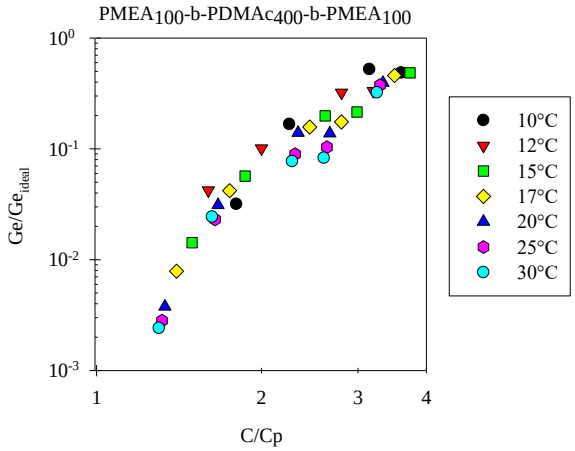

Figure 3. a) G_e/G_{e_ideal} as a function of the polymer concentration (g/L) at different temperatures (°C); b) G_e/G_{e_ideal} as a function of C/C_p at different temperatures (°C) for $PMEA_{100}$-b-$PDMAc_{400}$-b-$PMEA_{100}$.

The evolution of G_e/G_{e_ideal} is qualitatively the same at different temperatures for x = 100 (Figure 3a, where G_{e_ideal} is defined in equation 6, see experimental part) and is consistent with the expected behavior of a transient polymer network: G_e increases with C above C_p as more and more chains

become part of the network[40,45]. The fact that the curves on Figure 3a do not superimpose at different T values implies that C_p varies with T, which explains why a vertical shift was required to construct the master curves. By appropriately estimating C_p values, which depend on T, the evolution of G_e/G_{e_ideal} falls on a single curve as a function of C/C_p, see Figure 3b. The same qualitative behavior was also observed for x = 50 and 200 (Figure S9 in SI), allowing the determination of C_p in mol/L (Figure 4a) and g/L (Figure 4b) as a function of T for different x. For a given x, C_p increases with T (it reaches a plateau at 20°C for x = 100). However, for a given T, C_p does not follow a systematic trend with x (no matter if expressed in g/L or mol/L). One possible reason to explain the variations of C_p as a function of T and x could be that N_{agg} varies with these parameters. Increasing N_{agg} indeed decreases the molar concentration of physical cross-linking points, which may therefore increase C_p expressed in mol/L. However, this cannot explain the increase of C_p with T for x = 100 and x = 200 as N_{agg} hardly varies in the relevant T-range (Figure 1). In addition, at T = 15°C, N_{agg} ~ 12, 60, 140 for, respectively, x = 50, 100, 200, whereas the molar percolation concentration does not follow a monotonous variation with x ($C_p = 2.10^{-4}$, 5.10^{-4} and 3.10^{-4} mol/L for x = 50, 100 and 200 respectively). The evolution of C_p with T and x therefore does not seem to be related to the extent of aggregation of the micelles, as was already reported for other BAB triblock copolymers[80].

a)

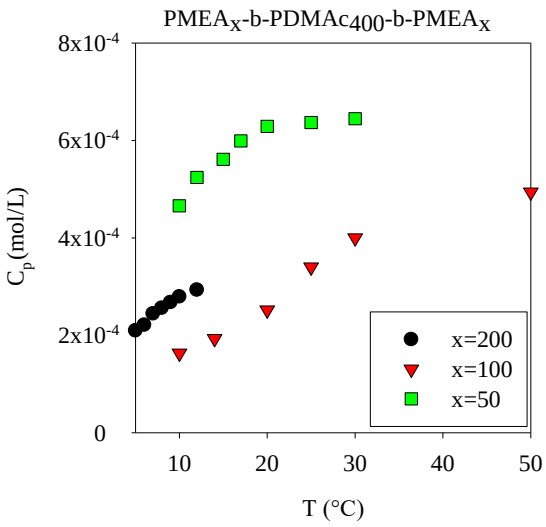

b)

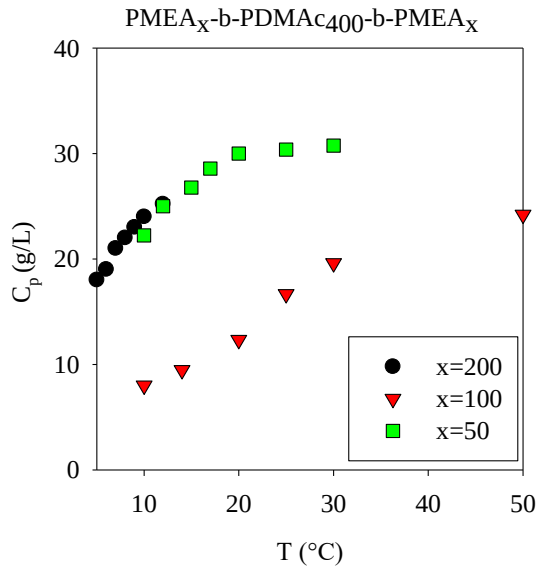

Figure 4. a) C_p in mol/L and b) C_p in g/L as a function of temperature (°C) determined for the three triblock copolymers, as indicated in the figures.

Quantitative evaluation of the exchange dynamics.

Within the investigated T-range, τ_r increases with increasing C for all x (Figure S10 in SI). This behavior is typical for self-assembling triblock copolymers and can be explained by the decrease of the percentage of defects in the network with increasing C, as discussed in the previous section. In particular, super-bridges relax more rapidly than one single elastically active chain[45,80]. As a consequence, the relaxation time measured by rheology gives a correct estimation of the exchange dynamics of the B blocks only for $C >> C_p$ where defects become negligible. Figure 5 compares the dependence of τ_r on temperature at C = 100 g/L, i.e. at $C >> C_p$, for the three x values. For a given temperature, the relaxation time strongly increases with x, in agreement with the fact that longer B blocks exchange more slowly. Indeed, longer B blocks are less mobile and exhibit a larger surface of contact with water, thereby increasing the energy barrier for unimer exchange and thus the exchange time[40,46-48]. In addition, for a given x value, τ_r increases strongly with increasing temperature. This key result is opposite to the expected behavior in case of a simple thermal-activation process (Arrhenius law), for which τ_r should decrease with T as explained in the introduction. This behavior implies that the energy barrier for the exchange of B blocks increases with T, which means that the PMEA block becomes less mobile/more hydrophobic with increasing T.

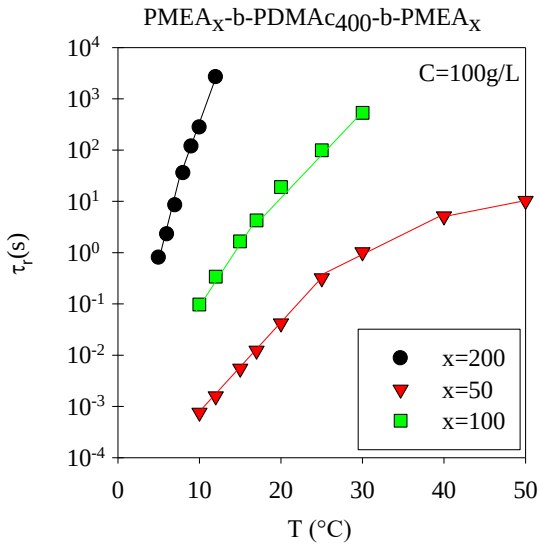

Figure 5. Relaxation time (s) as a function of temperature (°C), for the three triblock copolymers, at a polymer concentration of 100g/L, as indicated in the figure. Lines are guides to the eye.

We hypothesize that the increase of the exchange time with T is due to a decrease of the hydration of the PMEA block. Many studies have been conducted to determine the interaction of water with PMEA and how this affects the crystallization of water. However, these studies were mostly conducted at temperatures below 0°C[61,62,65,70,71,74,75]. PMEA being water-insoluble at room temperature, the evolution of its hydration with temperature above 0°C has seldom been studied. Mochizuki et al.[72] performed a ^{2}D NMR study revealing that PMEA still contains about 10 wt% water between 15 and 45°C and that the water is heterogeneously distributed within the polymer. Hou et al.[73] prepared statistical copolymers consisting of 90 mol% MEA and 10 mol% oligo (ethylene glycol)acrylate (OEGA 480 containing 8-9 ethylene oxide units per monomer) and observed a progressive, rather than abrupt, decrease of the hydration of the copolymer with increasing temperature. Similarly, it was observed[84] that nanogels of P(MEA-*co*-OEGA480) shrink in water with increasing temperature due to water expulsion. Interestingly, for this kind of nanogels, the evolution of the shrinkage with temperature was progressive rather than

critical[52,85,86], suggesting a gradual rather than abrupt variation of the hydrophobic character/hydration. These results, although they were not conducted with pure PMEA, agree with the gradual increase of the relaxation time observed in our study for the $PMEA_x$-*b*-$PDMAc_{400}$-*b*-$PMEA_x$ triblock copolymers. We stress that this behavior is very different from that of poly(*N*-isopropyl acrylamide) which abruptly dehydrates at its LCST, causing a critical sol-gel transition at the LCST.

Considering that the variation of the hydration of the PMEA blocks most probably explains the evolution of the exchange time of the B blocks with T, we compared the behavior of $PMEA_{100}$-*b*-$PDMAc_{400}$-*b*-$PMEA_{100}$ in D_2O and H_2O. D_2O-D_2O interactions have been reported by Schvartzman et al.[87] to be stronger than H_2O-H_2O interactions, which should make D_2O a poorer solvent for neutral polymers solubilized by hydrogen bonding with water. The authors consistently observed an increase of micelle aggregation number in D_2O compared to H_2O for PEO-*b*-PPO-*b*-PEO triblock copolymers. Surprisingly though, chemically cross-linked nanogels of P(MEA-co-OEGA 480) containing 90 mol% of MEA swelled more in D_2O than in H_2O according to Hou et al.[84]; which is in disagreement with the findings by Schvartzman et al. Additionally, the variation of the swelling of these nanogels with temperature was steeper in D_2O than in H_2O.

Light scattering experiments conducted with $PMEA_{100}$-*b*-$PDMAc_{400}$-*b*-$PMEA_{100}$ at 3 g/L and 20°C showed that R_h was not significantly different in H_2O and D_2O (23 nm in H_2O vs. 25 nm in D_2O), but that N_{agg} was slightly larger in D_2O (45) than in H_2O (37). Rheological experiments (Figure 6) showed longer relaxation times in D_2O than in H_2O, whereas G_e was unaffected. Moreover, the evolution of these parameters with T is identical. Our results are thus consistent with those of Schvartzman et al.[87] suggesting that PMEA is less hydrated in D_2O than in H_2O, causing an increase of the extent of aggregation and of the exchange time of the B blocks.

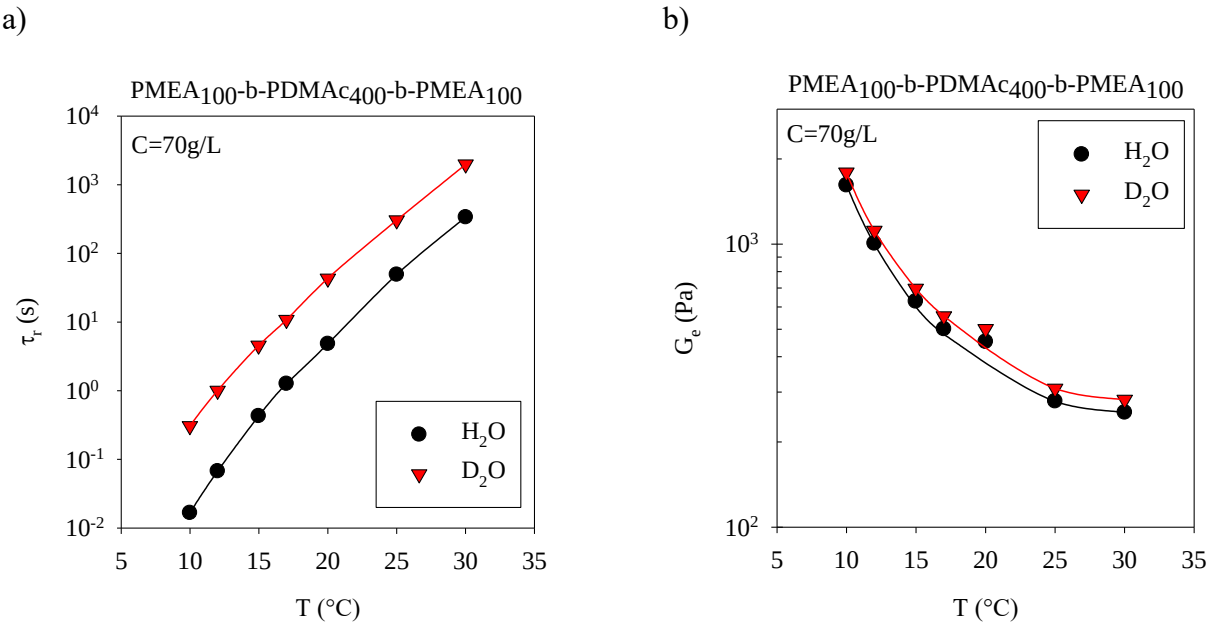

Figure 6. a) Relaxation time (s) as function of temperature (°C); b) elastic modulus (Pa) as function of temperature (°C) in H_2O and D_2O, for $PMEA_{100}$-b-$PDMAc_{400}$-b-$PMEA_{100}$ at 70 g/L. Lines are guides to the eyes.

2.3. Evidence for a critical reorganization temperature T_c

As briefly mentioned in the beginning of section 2.2, the transient network was found to reorganize above a critical temperature T_c, which varied with x. A typical rheological signature is presented in Figure 7 for x = 100 at 50 g/L and f=1Hz. Upon heating the aqueous dispersion from 10 to 30°C (< T_c), G' and G" varied only during the first 20s required to reach the target temperature and then remained constant even for long periods of time (data not shown), implying no specific behavior. Up to 30°C, the rheological properties were moreover reversible: full recovery was observed by heating from 10 to 30°C and shortly after cooling back down to 10°C (see Figure S11 in SI). On the contrary, upon heating from 10 to 50°C (> T_c), which takes about 1 minute, an abrupt

drop of G' and G" was observed after ~30 s followed by a subsequent increase after 2 min (Figure 7 and Figure S12). Moreover, G' and G" slowly continued to evolve with time afterwards even for days (data not shown). After cooling back from 50 to 10°C, which takes about 10 minutes, the initial rheological properties of the system at 10°C are not recovered (see SI Figure S13). The variations of G_e and τ_r after returning back to 10°C were moreover not reproducible. In some cases, applying a strong shear (30s at 100 rad/s, for a few minutes) helped recovering partially the initial properties (see SI Figure S14), but in other cases even shearing was not efficient (see SI Figure S13).

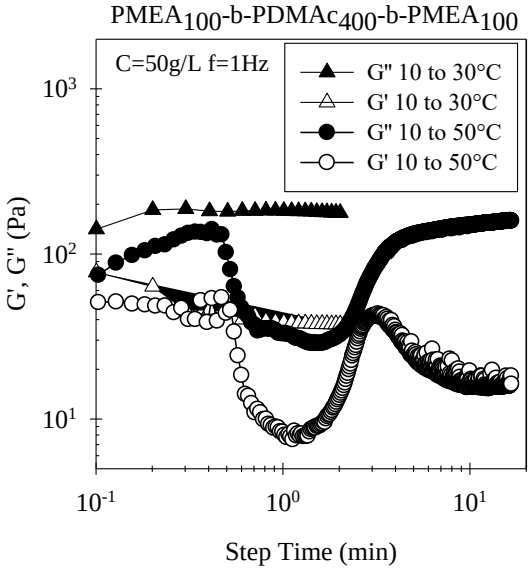

Figure 7. Time dependence of the storage (opened symbols) and loss moduli (filled symbols) while heating from 10°C to 30°C (< T_c) or to 50°C (>T_c), for $PMEA_{100}$-*b*-$PDMAc_{400}$-*b*-$PMEA_{100}$ at 50 g/L, f = 1 Hz. The target temperature was reached after about 1 min for T=30°C and about 1min30s for T=50°C. Lines are guides to the eyes. Notice that heating was done at a very fast rate so that the temperature was already higher than 10°C at the time of the first measurement.

Upon heating a sample from 10°C to a temperature $T > T_c$, the larger the difference between T and T_c, the larger the decrease of G' and G" and the slower the subsequent increase of G' and G" (see Figures 7 and S12 for representative examples). Qualitatively, the behavior is the same at different concentrations and different x, but quantitative differences are observed (see SI Figures S15 and S16). The amplitude of the variation of G' and G" during restructuration of the network increases with increasing C (Figure 8), whereas T_c decreases with increasing x. T_c was found to be between 40-50°C for x = 50, 30-40°C for x = 100 and 12-15°C for x = 200 (see details in SI, section 2.3.).

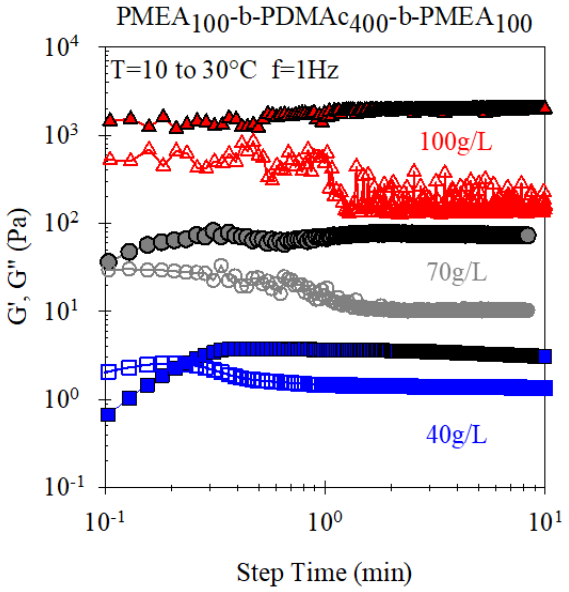

Figure 8. Time dependence of the storage (filled symbols) and loss moduli (opened symbols) while heating from 10°C to 30°C (< T_c) at different polymer concentrations (g/L), for $PMEA_{100}$-*b*-$PDMAc_{400}$-*b*-$PMEA_{100}$. The target temperature was reached after about 1 min for all measurements. Lines are guides to the eyes.

There is no abrupt variation of N_{agg} close to T_c at steady-state (Figure 1). Moreover, no significant dynamic variation of N_{agg} was observed by SLS during the time-span of the transition at T_c after heating $PMEA_{100}$-*b*-$PDMAc_{400}$-*b*-$PMEA_{100}$ from 10 to 50°C (data not shown). It follows that the molar concentration of micelles hardly changes close to T_c both at steady-state and over time. Therefore, the abrupt decrease of G' and G" at T_c cannot be explained by an abrupt variation of the number of elastically active chains. It is therefore probably caused by many of the bridging chains becoming temporarily more dynamic at T_c, so that they can relax rapidly and are able to reorganize. The subsequent increase of G' and G" implies that the system probably becomes again less dynamic. However, Figure 9 shows that if the same experiment is conducted at f = 0.1 or 10 Hz instead of 1 Hz, the behavior is qualitatively similar. It follows that when T_c is crossed, the number of elastically active chains does not vary, but some of them become so dynamic that they relax even at 0.1 Hz, causing an abrupt decrease of G', allowing the network to reorganize. The temperature at which this phenomenon occurs depends on x and the speed of the reorganization decreases with increasing temperature above T_c. According to those findings, we speculate that the transition is initiated when the dehydration of the core has reached a critical value during heating.

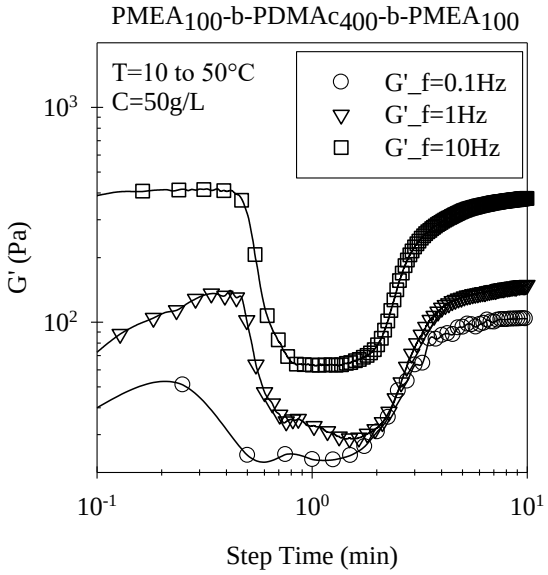

Figure 9. Time dependence of the elastic modulus (Pa) while heating above T_c (10 to 50°C) at different frequencies (Hz) for $PMEA_{100}$-*b*-$PDMAc_{400}$-*b*-$PMEA_{100}$ at 50 g/L. The target temperature was reached after about 1 min 30s for all measurements. Lines are guides to the eyes.

Conclusion

$PMEA_x$-*b*-$PDMAc_{400}$-*b*-$PMEA_x$ triblock copolymers form in aqueous solution small micelles at low concentrations and transient hydrogels above a critical percolation concentration.

Unexpectedly, an abrupt reorganization of the transient networks was observed above a critical temperature, T_c. The reorganization was characterized by an abrupt decrease of G' and G'' shortly after reaching T_c, followed by their recovery after a few minutes. This phenomenon was caused by a large fraction of elastically active chains becoming transiently very dynamic. The transition might be initiated by dehydration during heating, but further investigation is required to understand the origin of the process on a molecular level. From a more practical point of view, this unprecedented reorganization phenomenon causes strong variations of the elastic modulus and

relaxation time of the network, which are not reproducible and most often irreversible even upon application of a strong shear to rejuvenate the network. This critical temperature decreases with increasing PMEA block length.

Below T_c, the behavior of the transient network is perfectly reproducible and the exchange time of the PMEA blocks between micellar cores could be determined by rheology. As expected, the exchange time increases for longer PMEA blocks, because the latter are less mobile and more hydrophobic. More originally, the exchange time increases strongly with increasing temperature, which is opposite to the classical arrhenian behavior and means that the activation energy increases with increasing temperature. A key result is that the variation of the exchange time with T is progressive (rather than abrupt as for PNIPAM which exhibits a critical sol-gel transition at its LCST), allowing fine-tuning of the rheological properties of the network with T. These results are attributed to the gradual dehydration of the thermo-sensitive PMEA-block with increasing temperature.

These findings are not only relevant to design thermo-thickening hydrogels based on PMEA, but they may also shed light on applications where PMEA is used, notably the design of blood-compatible hydrogels or the synthesis of self-assembled particles consisting of a PMEA core by Polymerization Induced Self-Assembly.

ASSOCIATED CONTENT

Supporting Information.

This material is available free of charge via the Internet at http://pubs.acs.org.

1. Synthesis of the $PMEA_x$-*b*-PDMAc400-*b*-$PMEA_x$ triblock copolymers; 2. Additional characterizations of the self-assembly in aqueous medium.

AUTHOR INFORMATION

Corresponding Author

*E-mail: olivier.colombani@univ-lemans.fr

Funding Sources

This work has been funded by the Agence Nationale de la Recherche in the framework of the DYNAMIC-PISA ANR project (ANR-19-CE06-0002-01).

Notes

The authors declare no competing financial interest.

ACKNOWLEDGMENT

This work has been funded by the Agence Nationale de la Recherche in the framework of the DYNAMIC-PISA ANR project (ANR-19-CE06-0002-01). The authors thank François Stoffelbach for his scientific support and help, Lazhar Benyahia and Cyrille Dechance for their help and support for the rheological measurements.

REFERENCES

1. K. Almdal; J. Dyre; S. Hvidt; O. Kramer. Towards a phenomenological definition of the term 'gel'. *Polym. Gels Netw.* **1993**, 1 (1), 5-17. DOI: https://doi.org/10.1016/0966-7822(93)90020-I.

2. M. Kempe; N. Scruggs; R. Verduzco; J. Lal; J. A. Kornfield. Self-assembled liquid-crystalline gels designed from the bottom up. *Nat. Mater.* **2004**, 3, 177-182. DOI: https://doi.org/10.1038/nmat1074.

3. R. J. Spontak; N. P. Patel. Thermoplastic elastomers: fundamentals and applications. *Curr. Opin. Coll. Interface Sci.* **2000**, 5 (5-6), 333-340. DOI: https://doi.org/10.1016/S1359-0294(00)00070-4

4. K. P. Mineart; C. Hong; L. A. Rankin. Decoupling of Mechanical and Transport Properties in Organogels via Solvent Variation. *Gels* **2021**, 7, 61. DOI: https://doi.org/10.3390/gels7020061.

5. E. R. Draper; D. J. Adams. Low-Molecular-Weight Gels: The State of the Art. *Chem. Commun.* **2017**, 3 (3), 390-410. DOI: https://doi.org/10.1016/j.chempr.2017.07.012.

6. J-M. Guenet. Physical Aspects of Organogelation: A Point of View. *Gels* **2021**, 7, 65. DOI: https://doi.org/10.3390/gels7020065.

7. P. C. Marr; A. C. Marr. Ionic liquid gel materials: applications in green and sustainable chemistry. *Green Chem.* **2016**, (1), 105-128. DOI: https://doi.org/10.1039/C5GC02277K

8. T. P. Lodge; T. Ueki. Mechanically Tunable, Readily Processable Ion Gels by Self-Assembly of Block Copolymers in Ionic Liquids. *Acc. Chem. Res.* **2016**, 49, 2107-2114. DOI: https://doi.org/10.1021/acs.accounts.6b00308.

9. T. Ueki. Stimuli-responsive polymers in ionic liquids. *Polym. J.* **2014**, 46, 646-655. DOI: 10.1038/pj.2014.37.

10. Z. Zhang; J. Hao. Bioinspired organohydrogels with heterostructures: Fabrications, performances, and applications. *Adv. Colloid Inter. Sci.* **2021**, 292, 102408. DOI: https://doi.org/10.1016/j.cis.2021.102408.

11. A. Singh; F.-I. Auzanneau; M. A. Rogers, Advances in edible oleogel technologies – A decade in review. *Food Res. Int.* **2017**, 97, 307-317.

12. X. Yang; A. Li; Y. Guo; L. Sun. Applications of mixed polysaccharide-protein systems in fabricating multi-structures of binary food gels—A review. *Trends Food Sci. Technol.* **2021**, 109, 197-210. DOI: https://doi.org/10.1016/j.tifs.2021.01.002.

13. Y. Cao; R. Mezzenga. Design principles of food gels. *Nat. Food* **2020**, 1, 106-118. DOI: https://doi.org/10.1038/s43016-019-0009-x.

14. Jeong, B.; Kimb, S. W.; Baeb, Y. H. Thermosensitive sol-gel reversible hydrogels. *Adv. Drug Delivery Rev.* **2002**, 54, 37-51, DOI: https://doi.org/10.1016/s0169-409x(01)00242-3.

15. Peppas, N. A.; Hilt, J. H.; Khademhosseini, A.; Langer, R. Hydrogels in Biology and Medicine: From Molecular Principles to Bionanotechnology. *Adv. Mater.* **2006**, 18, 1345-1360. DOI: 0.1002/adma.200501612.

16. Drury, J. L.; Mooney, D. J. Hydrogels for tissue engineering: scaffold design variables and applications *Biomaterials* **2003**, 24, 4337-4351. DOI: 10.1016/S0142-9612(03)00340-5.

17. Liu, J.; Qu, S.; Suo, Z.; Yang, W. Functional Hydrogel Coatings. *Natl. Sci. Rev.* **2020,** 8. DOI: 10.1093/nsr/nwaa254.

18. Dimitrov, I.; Trzebickab, B.; Müllerc, A. H. E.; Dworakb, A.; Tsvetanov, C. B. Thermosensitive water-soluble copolymers with doubly responsive reversibly interacting entities. *Prog. Polym. Sci.* **2007**, 32, 1275-1343. DOI: 10.1016/j.progpolymsci.2007.07.001.

19. C.Tsitsilianis. Responsive reversible hydrogels from associative "smart" macromolecules. *Soft Matter* **2010**, 6, 2372-2388. DOI: 10.1039/b923947b.

20. Chassenieux, C.; Tsitsilianis, C. Recent trends in pH/thermo-responsive self-assembling hydrogels: from polyions to peptides-based polymeric gelators. *Soft Matter* **2016**, 12, 1344-1359. DOI: 10.1039/c5sm02710a.

21. H. J. Moon; D. Y. Ko; M. H. Park; M. K. Joo; B.. Jeong. Temperature-responsive compounds as in situ gelling biomedical materials. *Chem. Soc. Rev.* **2012**, 41, 4860-4883. DOI: https://doi.org/10.1039/C2CS35078E

22. B. Jeong; S. W. Kim; Y. H. Bae. Thermosensitive sol-gel reversible hydrogels. *Adv. Drug Delivery Rev.* **2012**, 64, 154-162. DOI: https://doi.org/10.1016/j.addr.2012.09.012.

23. Z. Wei; J. H. Yang; J. Zhou; F. Xu; M. Zrinyi; P. H. Dussault; Y. Osada; Y. M. Chen. Self-healing gels based on constitutional dynamic chemistry and their potential applications. *Chem. Soc. Rev.* **2014**, (23), 8114-8131. DOI: https://doi.org/10.1039/C4CS00219A

24. D. Y. Ko; U. P. Shinde; B. Yeon; B. Jeong. Recent progress of in situ formed gels for biomedical applications. *Prog. Colloid Polym. Sci.* **2013**, 38, 672-701. DOI: https://doi.org/10.1016/j.progpolymsci.2012.08.002.

25. X. Cheng; J. Pan; Y. Zhao; M. Liao; H. Peng. Gel Polymer Electrolytes for Electrochemical Energy Storage. *Adv. Energy Mater.* **2018**, 8, 1702184. DOI: https://doi.org/10.1002/aenm.20170218.

26. M. Zhu; J. Wu; Y. Wang; M. Song; L. long; S. H. Siyal; X. Yang; G. Sui. Recent advances in gel polymer electrolyte for high-performance lithium batteries. *J. Energy Chem.* **2019**, 37, 126-142. DOI: https://doi.org/10.1016/j.jechem.2018.12.013.

27. D. Zhu; B. Bai; J. Hou. Polymer Gel Systems for Water Management in High-Temperature Petroleum Reservoirs: A Chemical Review. *Energy Fuels* **2017**, 31 (12), 13063-13087. DOI: https://doi.org/10.1021/acs.energyfuels.7b02897.

28. S. S. Babu; S. Prasanthkumar; A. Ajayaghosh. Self-Assembled Gelators for Organic Electronics. *Angew. Chem. Int. Ed.* **2012**, 51 (8), 1766 - 1776. DOI: 10.1002/anie.201106767.

29. A. Y-Y Tam; V. W-W. Yam. Recent advances in metallogels. *Chem. Soc. Rev.* **2013**, 42, 1540-1567. DOI: 10.1039/c2cs35354g.

30. S. Panja; D. J. Adams. Stimuli responsive dynamic transformations in supramolecular gels. *Chem. Soc. Rev*. **2021**, 50, 5165-5200. DOI: 10.1039/d0cs01166e.

31. P. R. A. Chivers; D. K. Smith. Shaping and structuring supramolecular gels. *Nat. Rev. Mater.* **2019**, 4, 463-478. DOI: https://doi.org/10.1038/s41578-019-0111-6.

32. Y. Lan; M. G. Corradini; R. G. Weiss; S. R. Raghavanc; M. A. Rogers. To gel or not to gel: correlating molecular gelation with solvent parameters. *Chem. Soc. Rev.* **2015**, 44, 6035-6058. DOI: 10.1039/c5cs00136f.

33. Y-F Li; Z. Li; Q. Lin; Y-W. Yang. Functional supramolecular gels based on pillar[n]arene macrocycles. *Nanoscale* **2020**, (4).

34. M. D. Segarra-Maset; V. J. Nebot; J. F. Miravet; B. Escuder. Control of molecular gelation by chemical stimuli. *Chem. Soc. Rev.* **2013**, 42, 7086. DOI: 10.1039/c2cs35436e.

35. A. Noro; M. Hayashi; Y. Matsushita. Design and properties of supramolecular polymer gels. *Soft Matter* **2012**, 8, 6416-6429. DOI: 10.1039/c2sm25144b.

36. L. Voorhaar; R. Hoogenboom. Supramolecular polymer networks: hydrogels and bulk materials. *Chem. Soc. Rev.* **2016**, 45, 4013-4031. DOI: 10.1039/c6cs00130k.

37. C. W. Peak; J. J. Wilker; G. Schmidt. A review on tough and sticky hydrogels. *Colloid. Polym. Sci.* **2013**, 291, 2031-2047

38. Q. Chen; H. Chen; L. Zhu; J. Zheng. Fundamentals of double network hydrogels. *J. Mater. Chem. B* **2015**, 3, 3654-3676. DOI: 10.1039/c5tb00123d.

39. T. Farjami; A. Madadlou. An overview on preparation of emulsion-filled gels and emulsion particulate gels. *Trends Food Sci. Technol.* **2019**, 86, 85-94. DOI: https://doi.org/10.1016/j.tifs.2019.02.043.

40. C. Chassenieux; T. Nicolai; L. Benyahia. Rheology of associative polymer solutions. *Curr. Opin. Colloid. Interface Sci.* **2011**, 16, 18-26. DOI: 10.1016/j.cocis.2010.07.007.

41. Winnik, M. A.; Yekta, A. Associative polymers in aqueous solutions. *Curr. Opin. Colloid. Interface Sci.* **1997**, 424-435.

42. B. Jeong; S. W. Kim; Y. H. Bae. Thermosensitive sol–gel reversible hydrogels. *Adv. Drug Delivery Rev.* **2002**, 54 (1), 37-51. DOI: https://doi.org/10.1016/S0169-409X(01)00242-3.

43. R. Tamate; HK. Hashimoto; T. Ueki; M. Watanabe. Block copolymer self-assembly in ionic liquids. *Phys. Chem. Chem. Phys.* **2018**, 20 (39), 25123-25139. DOI: https://doi.org/10.1039/C8CP04173C.

44. M. J. Taylor; P. Tomlins; T. S. Sahota. Thermoresponsive Gels. *Gels* **2017**, 3 (1), 4. DOI: https://doi.org/10.3390/gels3010004.

45. Annable, T.; Buscall, R.; Ettelaie, R.; Whittlestone, D. The rheology of solutions of associating polymers: Comparison of experimental behavior with transient network theory. *J. Rheol.* **1993**, 37, 695-726. DOI: 10.1122/1.550391.

46. Zinn, T.; Willner, L.; Lund, R. Telechelic Polymer Hydrogels: Relation between the Microscopic dynamics and Macroscopic Viscoelastic Response. *ACS Macro Lett.* **2016**, 5, 1353-1356. DOI: 10.1021/acsmacrolett.6b00824.

47. A. Halperin. On micellar exchange: The Role of the Insertion Penalty. *Macromolecules* **2011**, 5072-5074. DOI: dx.doi.org/10.1021/ma200811x.

48. Nicolai, T.; Colombani, O.; Chassenieux, C. Dynamic polymeric micelles versus frozen nanoparticles formed by block copolymers. *Soft Matter* **2010**, 6, 3111-3118. DOI: 10.1039/b925666k.

49. Mistry, D.; Annable, T.; Yuan, X.-F.; Booth, C. Rheological Behavior of Aqueous Micellar Solutions of a Triblock Copolymer of Ethylene Oxide and 1,2-Butylene Oxide: B10E410B10. *Langmuir* **2006**, 22, 2986-2992. DOI: 10.1021/la0532205.

50. Tsitsilianis, C.; Serras, G.; Ko, C.-H.; Jung, F.; Papadakis, C. M.; Rikkou-Kalourkoti, M.; S., P. C.; Schweins, R.; Chassenieux, C. Thermoresponsive Hydrogels Based on Telechelic Polyelectrolytes: From Dynamic to "Frozen" Networks. *Macromolecules* **2018**, 51, 2169-2179. DOI: 10.1021/acs.macromol.8b00193.

51. Lauber, L.; Santarelli, J.; Boyron, O.; Chassenieux, C.; Colombani, O.; Nicolai, T. pH- and Thermoresponsive Self-Assembly of Cationic Triblock Copolymers with Controlled Dynamics. *Macromolecules* **2017**, 50, 416-423. DOI: 10.1021/acs.macromol.6b02201.

52. A. D. Drozdov. Equilibrium Swelling of Biocompatible Thermo-Responsive Copolymer Gels. *Gels* **2021**, 7 (2), 40. DOI: https://doi.org/10.3390/gels7020040.

53. Hietala, S.; Nuopponen, M.; Kalliomäki, K.; Tenhu, H. Thermoassociating Poly(N-isopropylacrylamide) A-B-A Stereoblock Copolymers. *Macromolecules* **2007** 41, 2627-2631. DOI: 10.1021/ma702311a.

54. Castelletto, V.; Hamley, I. W.; Yuan, X.-F.; Kelarakisc, A.; Booth, C. Structure and rheology of aqueous micellar solutions and gels formed from an associative poly(oxybutylene)-poly(oxyethylene)-poly(oxybutylene) triblock copolymer. *Soft Matter* **2005**, 1, 138-145. DOI: 10.1039/b419103j.μ

55. Podhajecka, K.; Prochazka, K.; Hourdet, D. Synthesis and viscoelastic behavior of water-soluble polymers modified with strong hydrophobic side chains. *Polymer* **2007**, 48, 1586-1595. DOI: 10.1016/j.polymer.2007.01.013.

56. Lutz, J.-F.; Akdemir, O.; Hoth, A. Point by Point Comparison of Two Thermosensitive Polymers Exhibiting a Similar LCST: Is the Age of Poly(NIPAM) Over? *J. Am. Chem. Soc.* **2006**, 128, 13046-13047. DOI: 10.1021/ja065324n.

57. Lutz, J.-F. Thermo-Switchable Materials Prepared Using the OEGMA-Platform. *Adv. Mater.* **2011**, 23, 2237-2243. DOI: 10.1002/adma.201100597.

58. N. Badi. Non-linear PEG-based thermoresponsive polymer systems. *Prog. Polym. Sci.* **2017**, 66, 57-79.

59. Vancoillie, G.; Frank, D.; Hoogenboom, R. Thermoresponsive poly(oligo ethylene glycol acrylates). *Prog. Polym. Sci.* **2014**, 39, 1074-1095.

60. Hoogenboom, R.; Zorn, A.-M.; Keul, H.; Barner-Kowollikc, C.; Moeller, M. Copolymers of 2-hydroxyethylacrylate and 2-methoxyethyl acrylate by nitroxide mediated polymerization: kinetics, SEC-ESI-MS analysis and thermoresponsive properties. *Polym. Chem.* **2012**, 3, 335-342. DOI: 10.1039/c1py00344e.

61. Tanaka, M.; Motomura, T.; Ishii, N.; Shimura, K.; Onishi, M.; Mochizuki, A.; Hatakeyama, T. Cold crystallization of water in hydrated poly(2-methoxyethyl acrylate) (PMEA). *Polym. Int.* **2000**, 49, 1709-1713.

62. Tanaka, M.; Mochizuki, A. Effect of water structure on blood compatibility—thermal analysis of water in poly(meth)acrylate. *J. Biomed. Mater. Res., Part A* **2004**, (4), 695.

63. Mizoue, Y.; Onodera, E.; Haraguchi, K.; Yusa, S.-i. Association Behavior of Amphiphilic ABA Triblock Copolymer Composed of Poly(2-methoxyethyl acrylate) (A) and Poly(ethylene

oxide) (B) in Aqueous Solution. *Polymers* **2022**, 14, 1678. DOI: https://doi.org/10.3390/polym14091678.

64. Kurokawa, N.; Endo, F.; Bito, K.; Maeda, T.; Hotta, A. Antithrombogenic poly(2-methoxyethyl acrylate) elastomer via triblock copolymerization with poly(methyl methacrylate). *Polymer* **2021**, 228. DOI: https://doi.org/10.1016/j.polymer.2021.123876.

65. Miwa, Y.; Ishida, H.; Tanaka, M.; Mochizuki, A. 2H-NMR and 13C-NMR Study of the Hydration Behavior of Poly(2-methoxyethyl acrylate), Poly(2-hydroxyethyl ethacrylate)and Poly(tetrahydrofurfuryl acrylate) in Relation30 to Their Blood Compatibility as Biomaterials. *J. Biomater. Sci., Polym. Ed.* **2010**, 21, 1911-1924. DOI: 10.1163/092050610X489682.

66. Bag, M. A.; Valenzuela, L. M. Impact of the Hydration States of Polymers on Their Hemocompatibility for Medical Applications: A Review. *Int. J. Mol. Sci.* **2017**, 18, 1422. DOI: https://doi.org/10.3390/ijms18081422.

67. Sato, K.; Kobayashi, S.; Kusakari, M.; Watahiki, S.; Oikawa, M.; Hoshiba, T.; Tanaka, M. The Relationship Between Water Structure and Blood Compatibility in Poly(2-methoxyethyl Acrylate) (PMEA) Analogues. *Macromol. Biosci.* **2015**, 15, 1296-1303. DOI: 10.1002/mabi.201500078.

68. Haraguchi, K.; Kubota, K.; Takada, T.; Mahara, S. Highly Protein-Resistant Coatings and Suspension Cell Culture Thereon from Amphiphilic Block Copolymers Prepared by RAFT Polymerization. *Biomacromolecules* **2014**, 1992-2003. DOI: https://doi.org/10.1021/bm401914c.

69. Haraguchi, K.; Takehisa, T.; Mizuno, T.; Kubota, K. Antithrombogenic Properties of Amphiphilic Block Copolymer Coatings: Evaluation of Hemocompatibility Using Whole Blood. *ACS Biomater. Sci. Eng.* **2015**, 1 (6), 352-362. DOI: 10.1021/acsbiomaterials.5b00079.

70. Morita, S.; Tanaka, M.; Kitagawa, K.; Ozaki, Y. Hydration Structure of Poly(2-methoxyethyl acrylate): Comparison with a 2-Methoxyethyl Acetate Model Monomer. *J. Biomater. Sci., Polym. Ed.* **2010**, 21, 1925-1935.

71. Morita, S.; Tanaka, M.; Ozaki, Y. Time-Resolved In Situ ATR-IR Observations of the Process of Sorption of Water into a Poly(2-methoxyethyl acrylate) Film. *Langmuir* **2007**, 23, 3750-3761. DOI: 10.1021/la0625998.

72. Mochizuki, A.; Miwa, Y.; Yahata, C.; Ono, D.; Kawaguchi, T. Water structure of poly(2-methoxyethyl acrylate) observed by nuclear magnetic resonance spectroscopy. *J. Biomater. Sci., Polym. Ed.* **2020**, 1024-1040.

73. Hou, L.; Wu, P. On the abnormal ‘‘forced hydration’’ behavior of P(MEA-co-OEGA) aqueous solutions during phase transition from infrared spectroscopic insights. *Phys. Chem. Chem. Phys.* **2016**, 18, 15593. DOI: 10.1039/c6cp01244b.

74. Gemmei-Ide, M.; Ohya, A.; Kitano, H. Recrystallization of Water in Non-Water-Soluble (Meth)Acrylate Polymers Is Not Rare and Is Not Devitrification. *J. Phys. Chem. B* **2012**, 116, 1850-1857.

75. Gemmei-Ide, M.; Kitano, H. Recrystallization of Water in a Non-Water-Soluble Polymer Examined by Fourier Transform Infrared Spectroscopy: Poly(2-methoxyethylacrylate) with Low Water Content. *J. Phys. Chem. B* **2008**, 112, 12863-12866. DOI: 10.1021/jp806973c.

76. Mellot, G.; Guigner, J.-M.; Bouteiller, L.; Stoffelbach, F.; Rieger, J. Templated PISA: Driving Polymerization-Induced Self-Assembly towards Fibre Morphology. *Angew. Chem. Int. Ed.* **2019**, (58), 3171-3177. DOI: 10.1002/anie.201809370.

77. Sugihara, S.; Ma'Radzi, A. H.; Ida, S.; Irie, S.; Kikukawa, T.; Maeda, Y. In situ nano-objects via RAFT aqueous dispersion polymerization of 2-methoxyethyl acrylate using poly(ethylene oxide) macromolecular chain transfer agent as steric stabilizer. *Polymer* **2015**, (76), 17-24.

78. Berne, B.; Pecora, R., Dynamic Light Scattering. *Wiley: New York*, **1976**.

79. Brown, W., Dynamic Light Scattering: The Method and Some Applications. Clarendon *Press: Oxford*, **1993**.

80. Charbonneau, C.; Chassenieux, C.; Colombani, O.; Nicolai, T. Controlling the Dynamics of Self-Assembled Triblock Copolymer Networks via the pH. *Macromolecules* **2011**, 44, 4487-4495. DOI: dx.doi.org/10.1021/ma2002382.

81. Seitz, M. E.; Burghardt, W. R.; Faber, K. T.; Shull, K. R. Self-Assembly and Stress Relaxation in Acrylic Triblock Copolymer Gels. *Macromolecules* **2007**, 40, 1218-1226. DOI: 10.1021/ma061993+.

82. Lund, R.; Willner, L.; Richter, D.; Iatrou, H.; Hadjichristidisc, N.; Lindner, P. Unraveling the equilibrium chain exchange kinetics of polymeric micelles using small-angle neutron scattering – architectural and topological effects. *J. Appl. Cryst*. **2007**, 40, 327-331.

83. Larson, R. G. The structure and Rheology of Complex fluids; *Oxford University Press*, **1999**.

84. Hou, L.; Ma, K.; An, Z.; Wu, P. Exploring the Volume Phase Transition Behavior of POEGA- and PNIPAM-Based Core−Shell Nanogels from Infrared-Spectral Insights. *Macromolecules* **2014**, 47, 1144-1154. DOI: dx.doi.org/10.1021/ma4021906.

85. Hou, L.; Wu, P. Microgels with Linear Thermosensitivity in a Wide Temperature Range. *Macromolecules* **2016**, 49, 6095-6100. DOI: 10.1021/acs.macromol.6b01359.

86. Liu, G.; Qiu, Q.; An, Z. Development of thermosensitive copolymers of poly(2-methoxyethyl acrylate-co-poly(ethylene glycol) methyl ether acrylate) and their nanogels synthesized by RAFT dispersion polymerization in water. *Polym. Chem.* **2012**, 2, 504-513. DOI: 10.1039/c2py00533f.

87. Schvartzman-Cohen, R.; Ren, C.-I.; Szleifer, I.; Yerushalmi-Rozen, R. An isotopic effect in self-assembly of amphiphilic block copolymers: the role of hydrogen bonds. *Soft Matter* **2009**, 5, 5003-5011. DOI: 10.1039/b913005e.